ECS Transactions, 50 (29) 5-15 (2013)
10.1149/05029.0005ecst ©The Electrochemical Society

Metal-Salens As Catalysts In Electroreductive Cyclization and Electrohydrocyclization: Computational and Experimental Studies

J.M. Yates, J.S. Fell, J.A. Miranda, and B.F. Gherman

Department of Chemistry, California State University, Sacramento
Sacramento, California 95819-6057, USA

The use of chiral Ni(II)-salen derivatives was examined in mediated electrohydrocyclization reactions. Cyclic voltammetry established the existence of a catalytic current. Bulk electrolysis revealed a slight change in the diastereoselectivity of the cyclizations. Computational studies were conducted that showed that Ni(II) and Zn(II) were the best metals for electron transfer, while the analogous Co(II) and Cu(II) compounds would likely not result in effective electron transfer.

Introduction

Electrochemistry provides a convenient tool with which electrons can be selectively introduced or removed from an organic molecule (1). It allows for the reversal of functional group polarity and can therefore produce umpolung reactions. This allows one to couple either two electrophiles or two nucleophiles in ways in which it would be otherwise impossible to accomplish. Electroreductive cyclization (ERC) refers to those processes wherein an electron-deficient alkene is tethered to an acceptor (e.g., an aldehyde or ketone) which undergoes an electrochemically promoted reductive cyclization leading to the formation of a new sigma bond between the β-carbon of the alkene and the acceptor unit. The electroreductive cyclization was pioneered in 1988 by Baizer, Little, and co-workers (2). Cyclic voltammetry firmly established that the α,β-unsaturated unit corresponded to the electrophore. Cyclization generally favored the formation of the product wherein the hydroxy and (methoxycarbonyl)methyl units were *trans* to one another. Sowell, Wolin, and Little used two electroreductive cyclizations during the formal total synthesis of quadrone (3). Electrohydrocyclization (EHC) refers to those processes which undergo an electrochemically promoted reductive cyclization leading to the formation of a new sigma bond between the β-carbons of α, β-unsaturated esters or nitriles. Moens, Baizer, and Little reported the use of an EHC reaction as a key step in the total synthesis of the natural product 1-sterpurene (4). The mechanism of the ERC reaction was investigated by Leonetti, Fry, and Little (5).

Miranda, Wade, and Little reported a variant of the ERC and EHC reaction that used catalytic Ni(II)-salen as a mediator (7). The transformations were achieved in yields ranging from 60% to 94% using either a mercury pool or environmentally preferable reticulated vitreous (RVC) cathode. The mechanism of mediated ERC and EHC reactions was also studied. The authors proposed the existence of a mechanistic continuum involving an equilibrium between Ni(II)-salen and two reduced forms, one being the metal-centered species **1**, the other being ligand-centered species **2**. In the ERC and EHC reactions, the ligand-centered species was theorized to be the dominant form of the reduced Ni(II)-salen. There is much support for the existence of **2**. Peters

discovered that the catalytic reduction of 1-iodooctane in the presence of "electrogenerated nickel(I) salen" led to the formation of products from the alkylation of one or both of the imino bonds of the salen ligand (7). They concluded that the reactive mediator that led to the alkylated products is best described by a ligand-centered species, namely Ni(II)-salen radical anion. In addition, reduced Ni(II)-salen radical anion displays an ESR spectrum that shows delocalization of spin onto the ligand.

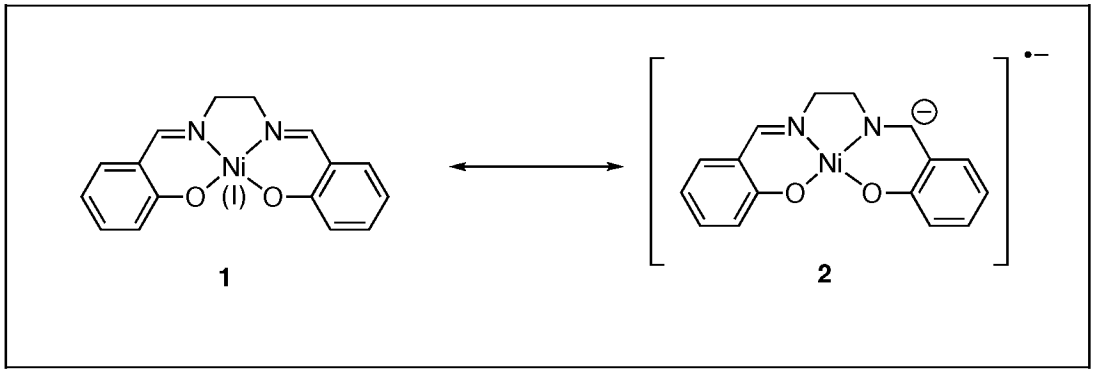

Figure 1. Reduced Ni(II)-salen (metal-centered anion vs. ligand centered anion).

In mediated ERC, while Ni(II)-salen (reduction potential or E_{pc} = -1.60 V vs Ag/AgCl) is an effective electrochemical mediator, the analogous Co(II)-salen (E_{pc} = -1.10 V vs Ag/AgCl) fails to promote cyclization. Direct ERC (unmediated) occurs at a reduction potential of -2.35 V vs. Ag/AgCl. It was concluded that the 1.25 V thermodynamic barrier was too large to allow electron transfer to occur from the reduced form of the Co(II) salen to the substrate (6). We sought to discover if there were other metal-salen compounds that also fall within an "electrochemical potential window" in which effective ERC would occur. Using density functional theory (DFT) calculations to predict electron affinities and cyclic voltammetry to experimentally measure reduction potentials for a wide variety of metal-salens, we were able to build a "training set" and "test set" of metal-salens. The correlation worked to accurately predict the test set to a mean signed error of -16 mV and a mean unsigned error of 99 mV (8).

Here, we also report our progress in the study of the mechanism of mediated ERC and EHC reactions. It was hoped that our investigation would not only provide insight into the mechanism, but also provide an entryway into the possibility of changing the structure of the salen ligand in order to promote asymmetric EHC reactions.

Results and Discussion

Computational Studies

The mechanism of electron transfer between reduced metal-salen and substrate was examined using computational chemistry methods. Metal-salens investigated included Ni(II)-, Zn(II)-, Co(II)-, and Cu(II)-salen, while substrates studied were acrylonitrile and methyl acrylate. Using density functional theory (DFT) calculations carried out with the Gaussian03 quantum chemistry program (9), the overall energy for the electron transfer reaction (ΔG°) between each reduced metal-salen and each substrate was determined.

The activation energy for electron transfer ($\Delta G_{et}^{\dagger}$) via an outer sphere (OS) mechanism was calculated according to Marcus Theory (10) (eqn 1), where λ is the

$$\Delta G_{et}^{\dagger} = \frac{\left(\Delta G^{\circ} + \lambda\right)^2}{4\lambda} \qquad [1]$$

reorganization energy. The reorganization energy accounts for both the internal reorganization energy of the acceptor and donor (λ_i) and the solvent reorganization energy (λ_0). The activation energy for electron transfer via an inner sphere (IS) mechanism was calculated using the free energy difference between reduced metal-salen and substrate reactants and the transition state for carbon-carbon bond formation between the ligand of the reduced metal-salen and the beta-carbon of the substrate (Figure 2).

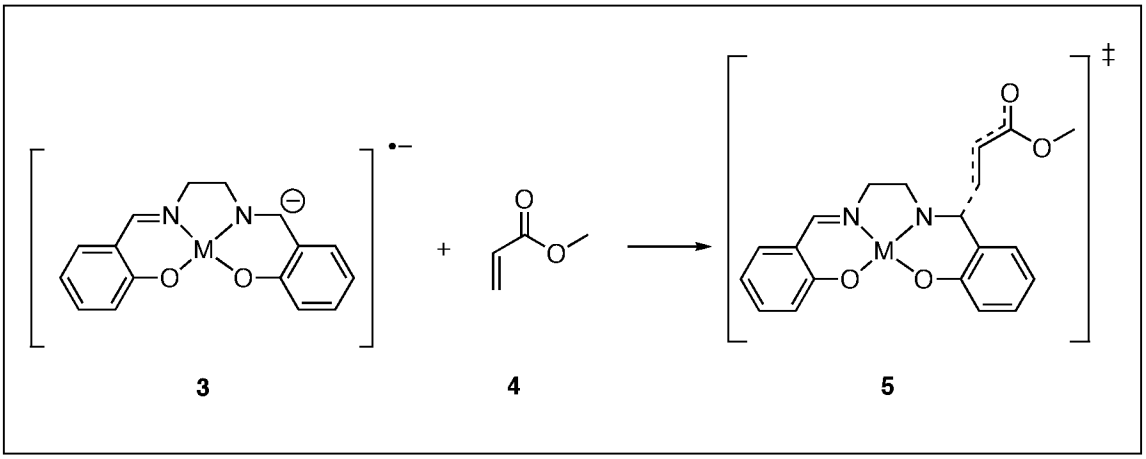

Figure 2. Mechanism for IS electron transfer, illustrating the transition state in the case of methyl acrylate as the substrate.

All DFT calculations utilized the B97-1 functional (11,12), which was previously demonstrated to optimally reproduce crystal structures and experimental electron affinities for Ni(II)-salens (8) and has also been shown to perform well for the prediction of 3d transition metal thermochemistry (13). Geometries were optimized using the 6-31G(d,p) basis set for all atoms, except for the metals for which the Stuttgart effective core potential basis was used (14). Final electronic energies were calculated using the optimized geometries and the 6-311++G(d,p) basis set on all atoms, except for the metals for which the Stuttgart effective core potential basis was used. Stationary points were verified as minima or transition states using vibrational frequency calculations, which also allowed for free energies to be calculated. Solvation energies in acetonitrile solvent were obtained using the IEF-PCM implicit solvation method as implemented in Gaussian03.

ΔG° values for the electron transfer reaction as well as free energies of activation for both the inner sphere and outer sphere electron transfer pathways are shown in Tables I and II. The order of thermodynamic favorability for the electron transfer by metal center (regardless of substrate) was found to be Zn(II) > Ni(II) » Co(II) > Cu(II). This order matched computed oxidation potentials for the reduced metal-salens, in which the

oxidation potentials for reduced Zn(II)- and Ni(II)-salen were found to be ~0.5 V higher than for reduced Co(II)- and Cu(II)-salen.

TABLE I. ΔG° and activation energies (25 °C; kcal/mol) for electron transfer with methyl acrylate as the substrate.

	ΔG°	**IS** $\Delta G_{et}^{\dagger}$	**OS** $\Delta G_{et}^{\dagger}$
Ni(II)-salen	-0.76	11.59	9.20
Zn(II)-salen	-1.91	12.91	8.53
Co(II)-salen	12.00	21.01	16.46
Cu(II)-salen	13.93	28.90	20.35

TABLE II. ΔG° and activation energies (25 °C; kcal/mol) for electron transfer with acrylonitrile as the substrate.

	ΔG°	**IS** $\Delta G_{et}^{\dagger}$	**OS** $\Delta G_{et}^{\dagger}$
Ni(II)-salen	-3.01	7.74	7.87
Zn(II)-salen	-4.16	8.34	7.44
Co(II)-salen	9.75	17.00	14.97
Cu(II)-salen	11.68	24.95	18.89

TABLE III. Electronic characterization of the reduced metal-salens.

	% metal character in LUMO	**Fukui nucleophilicity of anionic carbon**
Ni(II)-salen	4.61%	0.065
Zn(II)-salen	0.95%	0.061
Co(II)-salen	45.57%	0.058
Cu(II)-salen	59.36%	0.030

Activation energies for electron transfer were generally lower for the outer sphere pathway (with the only exception being Ni(II)-salen with acrylonitrile being ~0.1 kcal/mol higher for the outer sphere pathway). Preference for OS versus IS electron transfer was smallest with Ni(II) and Zn(II), in which cases reduction of the metal-salen is most ligand-based. On the other hand, the difference in $\Delta G_{et}^{\dagger}$ between OS and IS pathways was greatest with Co(II) and Cu(II), in which cases reduction of the metal-salen is most metal-based. Ligand-centered reduction of the neutral metal-salens was distinguished from metal-centered reduction by examination of the LUMO for the neutral metal-salen (Table III), which showed a large degree of metal character for Co(II) and Cu(II), and little to no metal character in the Ni(II) and Zn(II) cases. Metal- versus ligand-centered reduction was further investigated by examining the change in charge at the metal center upon reduction of the neutral-salen, showing that the partial charge of the metal appreciably decreased only in the case of reducing the Co(II)- and Cu(II)-salens.

Within the IS pathway, kinetic preference for electron transfer followed in the order Ni(II) > Zn(II) » Co(II) >Cu(II). The IS pathway relies on the presence of the formal carbanion on the ligand of the reduced metal-salen (Figure 2). That the IS pathway is most favorable for the Ni(II) and Zn(II) cases where reduction of the metal-salen is ligand-based follows logically. The IS pathway can likewise be viewed as a reaction

between the nucleophilic carbanion and the electrophilic substrate. Computed Fukui nucleophilicities (15) for the anionic carbon in the reduced metal-salens (Table III) showed the Ni(II) and Zn(II) cases to be more nucleophilic and therefore more reactive than the Co(II) and Cu(II) cases.

Within the OS pathway, kinetic preference for electron transfer followed in the order Zn(II) > Ni(II) » Co(II) >Cu(II). As the OS pathway relies on ability of the reduced metal-salen to transfer away an electron to the substrate, the trend here mirrors that for the overall reaction in following the oxidation potentials for the reduced metal-salens.

Cyclic Voltammetry (CV)

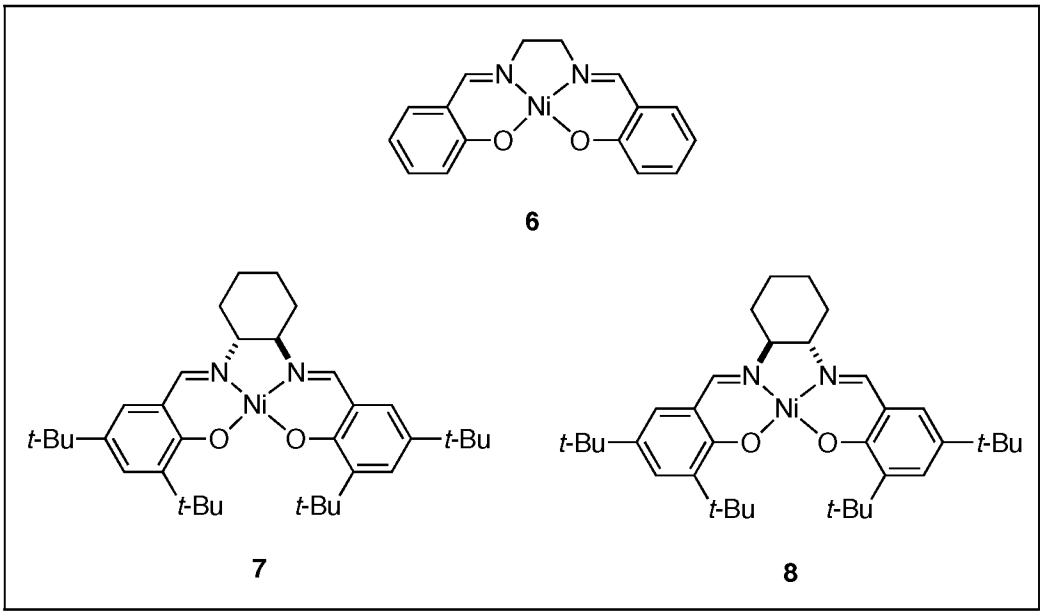

Figure 3. Ni(II)-salen **6** and chiral Ni(II)-salen derivatives **7** and **8**.

In order to investigate the mechanism of the mediated EHC reaction, we elected to study the various Ni(II)-salen compounds shown in Figure 3. These compounds include the parent Ni(II)-salen **6**, the chiral (R,R) Ni(II)- salen **7**, and the chiral (S,S) Ni(II)-salen **8**. The cyclic voltammetry results of the various Ni(II)-salen compounds in the presence of EHC substrate **9** are shown in Figures 4, 5, and 6. The cyclic voltammetry results of EHC substrate **9** are shown in Figure 7.

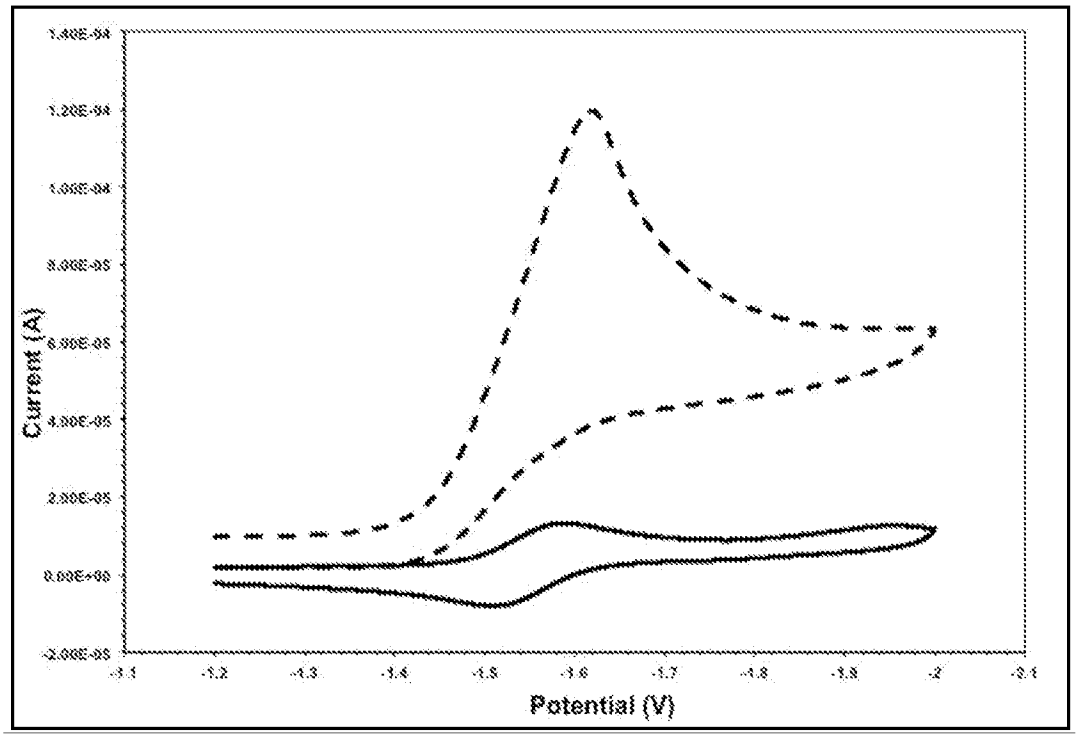

Figure 4. Cyclic voltammetry of 1 mM Ni(II)-salen **6** (solid line) in DMF and 1 mM Ni(II)-salen **6** with 10 mM EHC substrate **9** (dashed line) in DMF. Scan rate = 0.1 V/sec.

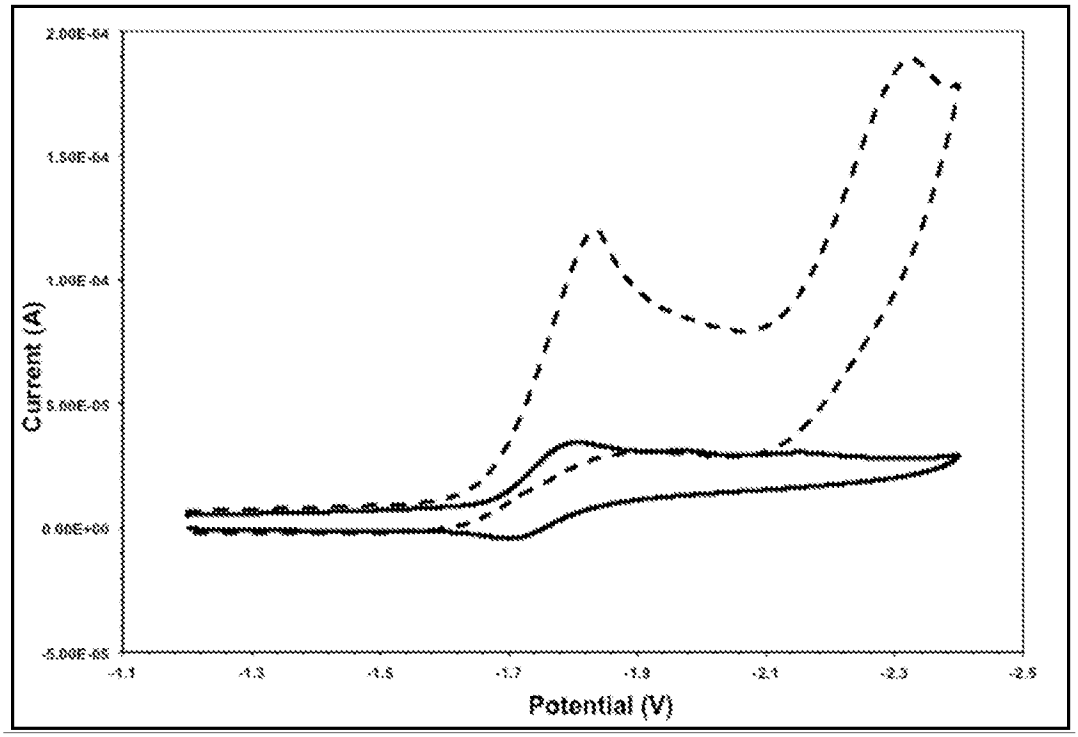

Figure 5. Cyclic voltammetry of 1 mM (R,R) Ni(II)-salen **7** (solid line) in DMF and 1 mM (R,R) Ni(II)-salen **7** with 10 mM EHC substrate **9** (dashed line) in DMF. Scan rate = 0.1 V/sec.

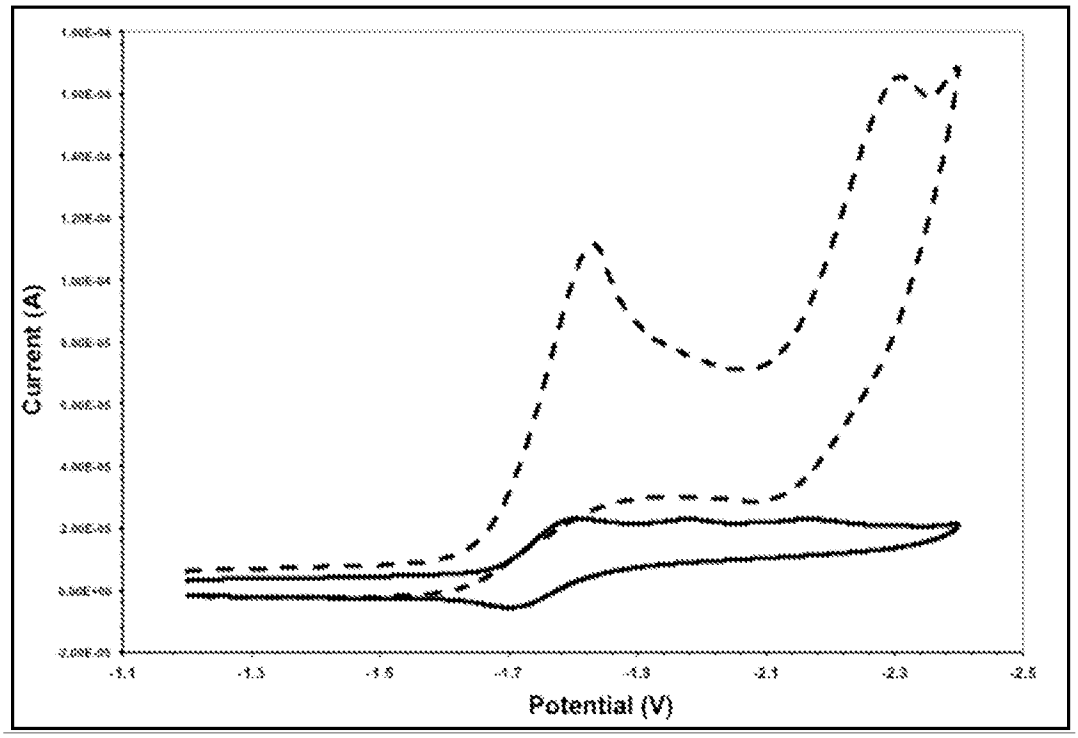

Figure 6. Cyclic voltammetry of 1 mM (S,S) Ni(II)-salen **8** (solid line) in DMF and 1 mM (S,S) Ni(II)-salen **8** with 10 mM EHC substrate **9** (dashed line) in DMF. Scan rate = 0.1 V/sec.

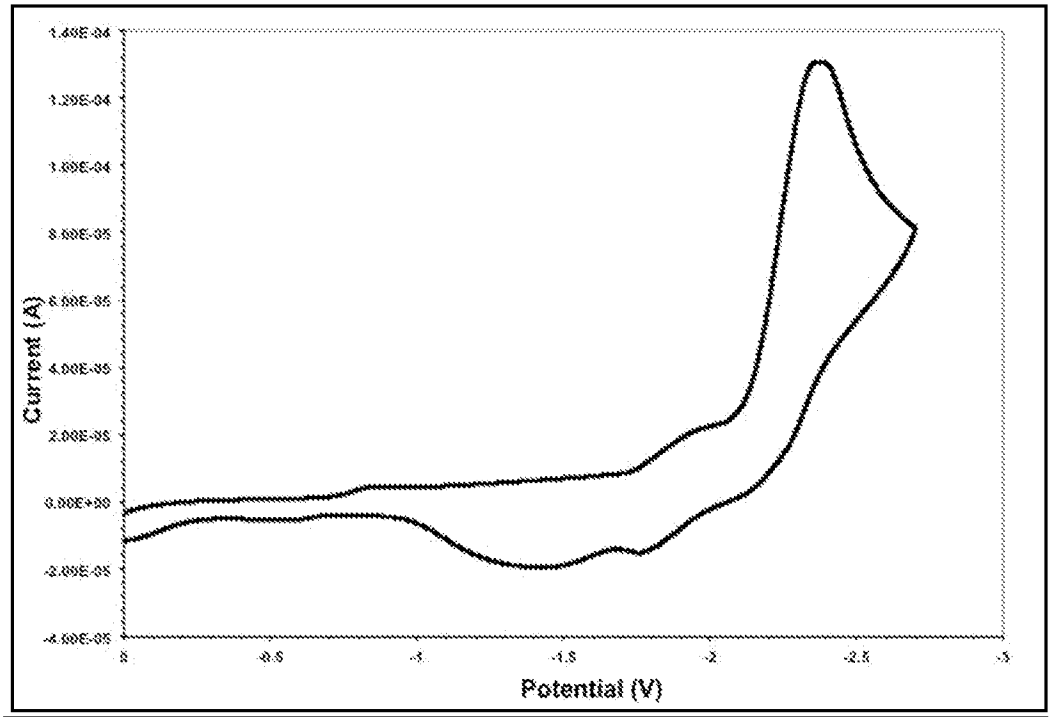

Figure 7. Cyclic voltammetry of 10 mM EHC substrate **9** in DMF. Scan rate = 0.1 V/sec.

Figure 7 showed that the EHC substrate exhibits an irreversible curve at -2.3 V. Each Ni(II)-salen compound exhibits a one-electron, reversible curve. Each Ni(II)-salen compound shows the presence of a significant amount of catalytic current. Observation of the catalytic current indicated that the substrate undergoes an irreversible reaction after reaction with the reduced catalyst.

Bulk electrolysis

In order to explore the effectiveness of the Ni(II)-salens shown above in mediated EHC reactions, we elected to perform bulk electrolysis reactions using EHC substrate **9** that would result in either *cis* cyclized diastereomer **10** or *trans* diastereomer **11**. The overall reaction is shown in Scheme 1. The reactions were performed at a reduction potential that ensured that the EHC substrate was not being directly reduced. The results of these experiments are summarized in Table 4.

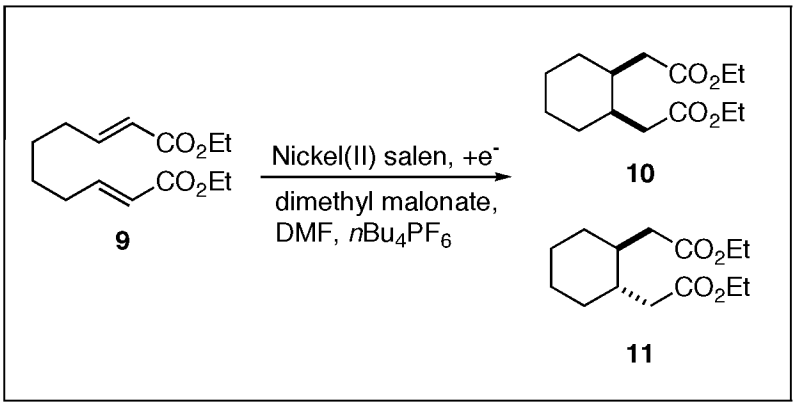

Scheme 1. Mediated electrohydrocyclization reactions using Ni(II)-salen derivatives.

TABLE IV. Bulk electrolysis reaction of Ni(II)-salens with EHC substrate **9**.

Ni(II)-salens	Reaction Yield	*Cis/Trans*
6	95.0 %	1/1.46
7	73.8 %	1/1.20
8	51.8 %	1/1.34

The results indicate that both chiral Ni(II)-salens are effective mediators in the EHC reaction. The parent Ni(II)-salen was shown to give the highest amount of *trans* cyclized product. Both chiral Ni(II)-salen catalysts gave lower selectivity and lower yields. This may indicate that the increased steric bulk of the substituents around the salen ligand lowers the reactivity of the catalyst when compared to an unsubstituted Ni(II)-salen.

Conclusion

Computational chemistry showed that electron transfer from various reduced metal-salens to both methyl acrylate and acrylonitrile was most thermodynamically favored with the Zn(II) and Ni(II) metal centers, while the free energies for electron transfer were considerably higher with the Co(II) and Cu(II) metal centers. Reduced Zn(II)- and

Ni(II)-salen also had significantly lower activation energies for electron transfer along both the inner-sphere (attributed to ligand-centered reduction of the neutral Zn(II)- and Ni(II)-salens) and outer-sphere pathways (attributed to the higher oxidation potentials of the reduced Zn(II)- and Ni(II)-salens).

Cyclic voltammetry established the existence of a catalytic current with Ni(II)-salen **6** and chiral Ni(II)-salens **8** and **9** when using EHC substrate **9**. Both chiral Ni(II)-salen catalysts proved to be effective electron transfer agents in mediated EHC reactions from bulk electrolysis. The diastereoselectivity of the cyclization always favored the *trans* product and was lower with the chiral catalysts. This may be due to the increased steric bulk of the chiral ligands preventing conjugate addition of the reduced complex to the EHC substrate.

We are currently investigating other Ni(II)-salen derivatives in mediated EHC reactions. These derivatives include a phenyl ring as a replacement for the ethyl bridge in Ni(II)-salen. We are also interested in investigating the catalytic behavior of Zn(II)-salen in mediated ERC and EHC reactions. The results of these experiments will be reported in due course.

Experimental

General

^{1}H Nuclear Magnetic Resonance (NMR) spectra were recorded using a Bruker 500 MHz Avance III spectrometer. ^{13}C NMR spectra were recorded using a Bruker 125 MHz Avance III spectrometer. An Agilent Technologies 7890A Gas Chromatography (GC)/Mass Spectrometry (MS) System containing an Agilent J&W GC column (stationary phase: Hp-5MS, 30 m x 0.250 mm x 0.25 μM) with a 5975 inert XL Ei/CI MSD with Triple-Axis Detector was used to obtain all GC/MS data. The method used for all runs was: 40 °C for 1 minute, 5°C/minute to 110 °C, 20 °C/minute to 280 °C, hold for 2 minutes.

(R,R)-(-)-N,N'-Bis(3,5-di-*tert*-butylsalicylidene)-1,2-cyclohexanediamine, 1,6 hexanediol, and dimethyl malonate were from Aldrich Chemical Company, Inc. 1,2 phenylenediamine, (ethoxycarbonylmethylene)triphenylphosphorane and sulfur trioxide-pyridine complex were from Alfa Aesar. Triethylamine (TEA), anhydrous tetrahydrofuran (THF), absolute ethanol (abs. EtOH), and anhydrous dimethylformamide (DMF) were from EMD. (S,S)-(+)-N,N'-Bis(3,5-di-*tert*-butylsalicylidene)-1,2-cyclohexanediamine was from Strem Chemicals. 3,5-di-*tert*-butylsalicylaldehyde, ethylenediamine, tetra-*n*-butylammonium hexaflourophosphate (nBu$_4$NPF$_6$) were from TCI Co.

Synthesis

EHC substrate **9** was made by Parikh-Doering oxidation of 1, 6 hexanediol, followed by *in situ* reaction with stabilized Wittig reagent (ethoxycarbonylmethylene)triphenylphosphorane (16, 17). The yellow oil was purified by flash chromatography on silica gel using 20:80 ethyl acetate/hexane as eluent to give EHC substrate **9** in 70.9 % overall.

All Ni(II)-salen derivative compounds were synthesized by a two step procedure (18).

Cyclic Voltammetry (CV)

A BASi C-3 Cell Stand and an Electrochemical Analyzer/Workstation, Model 600D, from CH Instruments were used for all electrochemical experiments. A standard single compartment glass cell vial was used for CV experiments. The working electrode was a glassy carbon electrode (surface area: 7 mm^2) and a platinum electrode was used as the auxiliary electrode (surface area: 2 mm^2). The potentials were recorded against a Ag/AgCl reference electrode, which was separated from the medium by a porous Vycor membrane (surface area: 28 mm^2). This electrode has a potential of -0.045 V versus the saturated calomel electrode (SCE) at 25 °C. The scan rate was 0.1 V/sec. All CVs were run in 0.1 M $n$$Bu_4PF_6$ in 5 mL of anhydrous dimethylformamide. The solution was deoxygenated for at least 10 minutes by bubbling nitrogen in the solution and the cell contents were maintained under a nitrogen atmosphere during the experiment. CV was performed using a computer-controlled potentiostat electroanalytical system. The data was collected and exported to a spreadsheet program.

Bulk Electrolysis

All reactions were carried out in a two compartment BE glass cell. The working electrode was a reticulated vitreous carbon (RVC) electrode (area: 31 cm^3). A coiled platinum wire (length: 23 cm) within a fritted glass isolation chamber was used as the auxiliary electrode. The reference electrode was Ag/AgCl, which was separated from the medium by a porous Vycor membrane (surface area 28 mm^2). This electrode has a potential of -0.045 V versus the saturated calomel electrode (SCE) at 25 °C.

A 0.1 M solution of $n$$Bu_4NPF_6$ in 85 mL of anhydrous DMF was poured into the cell containing all three electrodes. The solution was deoxygenated for 20 minutes by bubbling nitrogen in the solution and the cell contents were maintained under a nitrogen atmosphere during the experiment. The solution was also stirred with a stirbar throughout the entire experiment. A pre-electrolysis potential, depending upon the mediator used, was applied and the current was monitored until a constant level. In a separate vial, a 6.55 mM solution of the EHC substrate **9** was prepared in a solution containing 0.1 M of $n$$Bu_4NPF_6$ in 5 mL of anhydrous DMF. To this solution 1 mM of the Ni(II)-salen mediator and 2 equivalents of dimethyl malonate were added.

After the pre-electrolysis, the current was stopped and the solution containing the EHC substrate **9** was added to the cell. The current flow was resumed by applying the same potential applied during the pre-electrolysis step. The reaction was monitored by gas chromatography (GC). Once complete, the solution was transferred to a round bottom flask and cooled to 0 °C. The reaction was quenched with 60 mL of H_2O, extracted with diethyl ether (3 x 60 mL). The combined organic layers were washed with brine (3 x 60 mL) and dried over Na_2SO_4. The solvent was removed by rotary evaporation to give the crude product. The cyclized product was analyzed by ^1H NMR, ^{13}C NMR, ^1H – ^1H DQF-COSY, ^{13}C DEPT, and ^1H – ^{13}C HSQC. ^{1}NMR and ^{13}C NMR matched previously published data (6). The cyclized product *cis/trans* ratio was analyzed by GC/MS.

Acknowledgments

We gratefully acknowledge the National Science Foundation for funding this work through a Major Research Instrumentation Grant (#0922676). We also thank California State University, Sacramento, College of Natural Science and Mathematics for their support of this research.

References

1. R.D. Little and K.D. Moeller, *Electrochem. Soc. Interface,* **11***(4)*, 36 (2002).
2. R.D. Little, D.P. Fox, L. Van Hijfte, R. Dannecker, G. Sowell, R.L. Wolin, L. Moens, and M.M. Baizer, *J. Org. Chem.,* **53***(10)*, 2287 (1988).
3. C.G. Sowell, R.L. Wolin, and R.D. Little, *Tetrahedron Lett.,* **31***(4)*, 485 (1990).
4. L. Moens, M.M. Baizer, and R.D. Little, *J. Org. Chem.,* **51***(23)*, 4497 (1986).
5. A.J. Fry, R.D. Little, and J. Leonetti, *J. Org. Chem.,* **59**(17) 5017 (1994).
6. J.A. Miranda, C.J. Wade, and R.D. Little, *J. Org. Chem.,* **70**(20), 8017 (2005).
7. P.W. Raess, M.S. Mubarak, M.A. Ischay, M.P. Foley, T.B. Jennermann, K. Raghavachari, and D.G. Peters, *J. Electroanal. Chem.,* **603**, 124 (2007).
8. S.B. Bateni, K.R. England, A.T. Galatti, H. Kaur, V.A. Mendiola, A.R. Mitchell, M.H. Vu, B.F. Gherman, and J.A. Miranda, *Beilstein J. Org. Chem.,* **5**, 82 (2009).
9. M. J. Frisch, G. W. Trucks, H. B. Schlegel, G. E. Scuseria, M. A. Robb, J. R. Cheeseman, J. J. A. Montgomery, T. Vreven, K. N. Kudin, J. C. Burant, J. M. Millam, S. S. Iyengar, J. Tomasi, V. Barone, B. Mennucci, M. Cossi, G. Scalmani, N. Rega, G. A. Petersson, H. Nakatsuji, M. Hada, M. Ehara, K. Toyota, R. Fukuda, J. Hasegawa, M. Ishida, T. Nakajima, Y. Honda, O. Kitao, H. Nakai, M. Klene, X. Li, J. E. Knox, H. P. Hratchian, J. B. Cross, V. Bakken, C. Adamo, J. Jaramillo, R. Gomperts, R. E. Stratmann, O. Yazyev, A. J. Austin, R. Cammi, C. Pomelli, J. W. Ochterski, P. Y. Ayala, K. Morokuma, G. A. Voth, P. Salvador, J. J. Dannenberg, V. G. Zakrzewski, S. Dapprich, A. D. Daniels, M. C. Strain, O. Farkas, D. K. Malick, A. D. Rabuck, K. Raghavachari, J. B. Foresman, J. V. Ortiz, Q. Cui, A. G. Baboul, S. Clifford, J. Cioslowski, B. B. Stefanov, G. Liu, A. Liashenko, P. Piskorz, I. Komaromi, R. L. Martin, D. J. Fox, T. Keith, M. A. Al-Laham, C. Y. Peng, A. Nanayakkara, M. Challacombe, P. M. W. Gill, B. Johnson, W. Chen, M. W. Wong, C. Gonzalez and J. A. Pople. *Gaussian 03, Revision D.01*, Gaussian, Inc., Wallingford, CT 2004.
10. R. A. Marcus, *Annu. Rev. Phys. Chem.,* **15**, 155 (1964).
11. F. A. Hamprecht, A. J. Cohen, D. J. Tozer and N. C. Handy, *J. Chem. Phys.,* **109**, 6264 (1998).
12. A. D. Becke, *J. Chem. Phys.,* **107**, 8554 (1997).
13. W. Jiang, M. L. Laury, M. Powell and A. K. Wilson, *J. Chem. Theory Comput.,* doi: 10.1021/ct300455e (2012).
14. M. Dolg, U. Wedig, H. Stoll and H. Preuss, *J. Chem. Phys.,* **86**, 866 (1987).
15. R. G. Parr and W. Yang *Density Functional Theory of Atoms and Molecules*, Oxford University Press, New York (1989).
16. J.P. Parikh and W.E. Doering, *J. Am. Chem. Soc.,* **89**, 5505 (1967).
17. G. Wittig and W. Haag, *Chem. Ber.*, **88**(11), 1654 (1955).
18. W.C. Gilbert, L.T. Taylor, and J.G. Dillard, *J. Am. Chem. Soc.,* **95**, 2477 (1973).